Density structure and buoyancy of the oceanic lithosphere revisited

J. C. Afonso,[1] G. Ranalli,[2] and M. Fernàndez[1]

Received 3 February 2007; revised 28 March 2007; accepted 4 April 2007; published 17 May 2007.

[1] The density structure of the lithospheric and sublithospheric oceanic mantle is assessed with an integrating methodology that incorporates mineral physics, geochemical, petrological, and geophysical data. Compressibility, partial melting, and compositional layering are considered in addition to the standard thermal modelling. The results indicate that due to differences in the degree of melt depletion and crust segregation, the depth-averaged density of old oceanic plates with thermal thicknesses of ~105 ± 5 km is always lower than the density of the underlying sublithospheric mantle. Moreover, representative depth-averaged density contrasts between the plate and the adiabatic mantle, $\overline{\Delta\rho}$, do not exceed values of ~40 kg m^{-3}, in contrast to what is assumed ($\overline{\Delta\rho}$ > 70 kg m^{-3}) in many geodynamic models. Thus, the role of $\overline{\Delta\rho}$ in triggering/assisting processes such as subduction initiation may be less critical than previously thought.
Citation: Afonso, J. C., G. Ranalli, and M. Fernández (2007), Density structure and buoyancy of the oceanic lithosphere revisited, *Geophys. Res. Lett.*, *34*, L10302, doi:10.1029/2007GL029515.

1. Introduction

[2] The oceanic lithosphere (hereafter OL) is commonly seen as the cold thermal boundary layer above an approximately adiabatic mantle. In this scenario, the main factor controlling the density structure and buoyancy of the plate as it moves away from the ridge is its thermal structure. Two closely related and widely held concepts within this framework are that mature OL develops greater average densities, $\overline{\rho}$, than those in the underlying asthenosphere (unstable density stratification), and that depth-averaged density contrasts between mature plates and the adiabatic mantle ($\overline{\Delta\rho} = \overline{\rho}_{plate} - \overline{\rho}_{adiab.\ mantle}$) can reach values $\gtrsim$ 70 kg m^{-3} [cf. *Schubert et al.*, 2001].

[3] In detail, the OL is not only a thermal, but also a chemical and a mechanical boundary layer. Its thermophysical properties depend ultimately on its major-element composition and equilibrium mineral assemblage, which in turn depend on temperature, pressure, composition of the original source (i.e., upper mantle that has not experienced partial melting), and degree of melt depletion experienced at the mid-ocean ridge (hereafter MOR). Although the pioneering work that set the basis for these concepts was developed more than 30 years ago, little further exploration into the problems of describing and quantifying the density structure of the OL was considered subsequently. In recent years, however, considerable advances in the knowledge of the chemical/petrological structure of the OL have resulted from improved thermodynamic computational simulations of the MOR system [e.g., *Asimow et al.*, 2001, 2004], quantitative melting models applied to abyssal peridotites [e.g., *Niu*, 1997; *Baker and Beckett*, 1999], and laboratory studies on melt extraction processes at high temperatures and pressures [e.g., *Walter*, 2003; *Schutt and Lesher*, 2006]. These studies now allow detailed compositional modelling of the MOR-OL system [e.g., *Hynes*, 2005; *Lee et al.*, 2005], which can be converted to consistent density models of OL upon appropriate combination with mineral physics modelling [e.g., *Afonso*, 2006].

[4] This paper presents a detailed density model of the OL, based on a new combined petrological/geophysical methodology that integrates the latest data on mineral physics, geochemistry, petrology, and geophysical information relevant to the first 300 km of depth. We then use this density model to estimate the negative buoyancy of an oceanic plate with respect to a reference adiabatic mantle. We show that in view of this new composition-pressure-temperature dependent model for OL, as well as those recently presented elsewhere [*Hynes*, 2005; *Afonso*, 2006], the widely accepted idea of mature plates with $\overline{\Delta\rho} \gtrsim$ 70 kg m^{-3} and more dense than the underlying asthenosphere requires a thoughtful re-examination, along with its implications for dynamic processes such as subduction initiation.

2. Methodology

[5] The density structure of the oceanic lithospheric-sublithospheric mantle down to 300 km depth is obtained in a two-step process (see the online supplementary material[1] for more information). The first step involves the modelling of the major element-composition and mineral assemblage of the OL after melt extraction at the MOR. This is done by assuming a particular melting model and applying experimentally constrained relations between amount of melt removed and residual mineral modes for peridotites. To explore the effects of different melting models on the density structure of OL, here we use two competing models: quasi-linear (hereafter QL) and non-linear (hereafter NL). The former follows the classic formulation of *Turcotte and Phipps Morgan* [1992]; the latter is a representative mean of several recent batch and fractional models within the "normal" pressure range $2.0 < P_o < 3.5$ GPa, where P_o is the pressure of intersection of the solidus [e.g., *Asimow et al.*,

[1]Institute of Earth Sciences "J. Almera," Consejo Superior de Investigaciones Científicas, Barcelona, Spain.
[2]Department of Earth Sciences and Ottawa-Carleton Geoscience Centre, Carleton University, Ottawa, Ontario, Canada.

0094-8276/07/2007GL029515$05.00

[1]Auxiliary material data sets are available at ftp://ftp.agu.org/apend/gl/2007gl029515. Other auxiliary material files are in the HTML.

2001]. It is numerically implemented as two linear functions intercepting at 1.25 GPa and given by: $F_1 = 25.83 - 16.66P$; $F_2 = 9.16 - 3.33P$, where F is the degree of partial melting [%], and P is pressure [GPa]. This model has parameters P_o = 2.75 GPa and P_f = 0.2 GPa, where P_f is the pressure at which melting stops. For melt removed/residual modes relations we use petrological models of abyssal peridotites [*Niu*, 1997, 2004] and experimental data on both spinel and garnet peridotites [*Schutt and Lesher*, 2006]. The original "pyrolitic" composition of the undepleted mantle is taken from *McDonough and Sun* [1995], which yields average modal fractions Ol/Opx/Cpx/Grt ~ 59/12/14/15.

[6] In the second step, a representative thermal structure is obtained iteratively by fitting predictions from a synthetic oceanic transect to reliable databases of geophysical observables (gravity and geoid anomalies, elevation, surface heat flow and seismic velocities). Considering in each iteration the resulting mineral assemblage, the density as a function of temperature, pressure, and composition is obtained for each constituent mineral (and for the mantle rock) by solving their full equations of state (EoS), corrected for thermal expansivity. We adopt the experimental results of *Klemme and O'Neill* [2000] for describing the spinel-garnet phase transition, whereas the plagioclase-spinel phase transition is fixed at P = 650 MPa.

[7] All pertinent equations are solved in a 2-D domain using the finite-element code LitMod [*Afonso*, 2006]. Since most of the thermodynamic parameters for relevant mantle minerals are well fitted with a third-order Birch-Murnaghan EoS corrected for thermal effects, here we adopt this EoS for computing compressions at upper mantle pressures and temperatures. The overall uncertainty in our density estimations is <10 kg m^{-3} (thermodynamic parameters and details on the methodology are included in the online supplementary material). Our method to calculate densities of peridotitic rocks has been compared with that presented by *Hacker and Abers* [2004]. Differences between these two methods are within the range ±5 kg m^{-3}.

3. Results

3.1. Density Structure

[8] The modelled transect has been constructed using geophysical observables as constraints to the final model, along a 1560 km-long transect perpendicular to the Mid-Atlantic ridge (westward, at 20° N lat). Since no information regarding the crustal structure is available, an average crustal thickness of 7 km was chosen for the whole profile. The fit to the observables and the thermal structure of the best fitting model are shown in Figure 1. The plate has a maximum thermal thickness (depth of the 1300°C isotherm) of ~106 km, in agreement with other recent estimations for OL [*McKenzie et al.*, 2005]. The density distributions obtained from this thermal structure for the two isentropic melting models are shown in Figure 2. The first noticeable feature is the relatively abrupt jump in density at the spinel-garnet transition, indicated by the (lower) dashed yellow line. Since this phase change is an exothermic reaction, it is slightly shifted towards deeper levels the closer it is to the MOR, where it reaches ~76 km depth. Within the spinel and plagioclase stability fields, different depletion models do not affect the density structure significantly, although its mean value is slightly larger in the NL case. The effect of different depletion models is also negligible when the plate has a thermal thickness <80 km. Figure 2 shows that the density inversion within the lithosphere due to conductive cooling is, as expected, more pronounced for the NL model than for the QL depletion model. This is more visible toward the older sections of the plate, where mantle density reaches values 3370 kg m^{-3} right beneath the spinel-garnet transition in the NL case. Within the garnet stability field, the QL case shows a thicker core of material with densities >3360 kg m^{-3} than in the NL case. This is a consequence of the different pressures (i.e., depths) at which melt depletion starts in these models (~65 and 90 km depth in the QL and NL model, respectively; see insets in Figure 2). Undepleted (more dense) mantle makes up the lower 40 km of the plate in the QL case. However, density does not reach values 3370 kg m^{-3}, as in the NL case.

[9] At 1500 km from the ridge (x = 0 in Figure 2), the depth-averaged density within the spinel stability field is roughly 3 kg m^{-3} greater in the NL case than in the QL case. Within the garnet stability field, however, the depth-averaged density is only slightly greater (~1 kg m^{-3}) in the QL case. Since the garnet stability field is thicker than the spinel stability field, these two opposite effects approximately cancel each other when averaged through the total thickness of the plate. For instance, the depth-averaged density of the oceanic plate, including a 7-km thick crust (average density ρ_c = 2900 kg m^{-3}), at 1500 km from the ridge, is ~3314 and 3315 kg m^{-3} for the QL and NL model, respectively. These values are for a model without the plagioclase stability field (dashed blue lines in Figure 2). If the phase transition (spinel-to-plagioclase) is assumed to be complete, the above figures become ~3310 and 3312 kg m^{-3} for the QL and NL model, respectively. In both cases, however, the depth-averaged density values of the oceanic plate are significantly smaller than the estimated average density of the sublithospheric mantle right beneath the plate (>3330 kg m^{-3}, Figure 2). In a recent work, *Hynes* [2005] obtained similar results for 1-D models, although his method for estimating the density of OL is different from the one used in this paper.

3.2. Buoyancy

[10] In order to identify which parts of the lithosphere contribute positively to its overall buoyancy and which ones would promote the development of an instability (i.e., positive $\Delta\rho$ values imply downward buoyancy and vice-versa) we construct vertical profiles of density contrasts between the present model and an adiabatic reference model (hereafter RM-SI), at three different ages (25, 50, and 90 Ma according to *McKenzie et al.*'s [2005] model). RM-SI has the composition of undepleted mantle, a potential temperature T_p = 1300°C, a geotherm following an adiabatic gradient of 0.4°C km^{-1} [cf. *Schubert et al.*, 2001], and includes phase transitions. Since in terms of relative buoyancy there are no significant differences between the QL and NL models, here we only consider the latter for illustrative purposes. Results are summarized in Figure 3. The crust clearly represents the main contribution to positive buoyancy at all ages. In fact, for the cases of a 50 and 90 Ma old plate, it is the only buoyant part of the lithosphere. This is not strictly the case for plates younger than ~35 Ma, where there exists a positive contribution near the base to the plate. This is due to the differences in

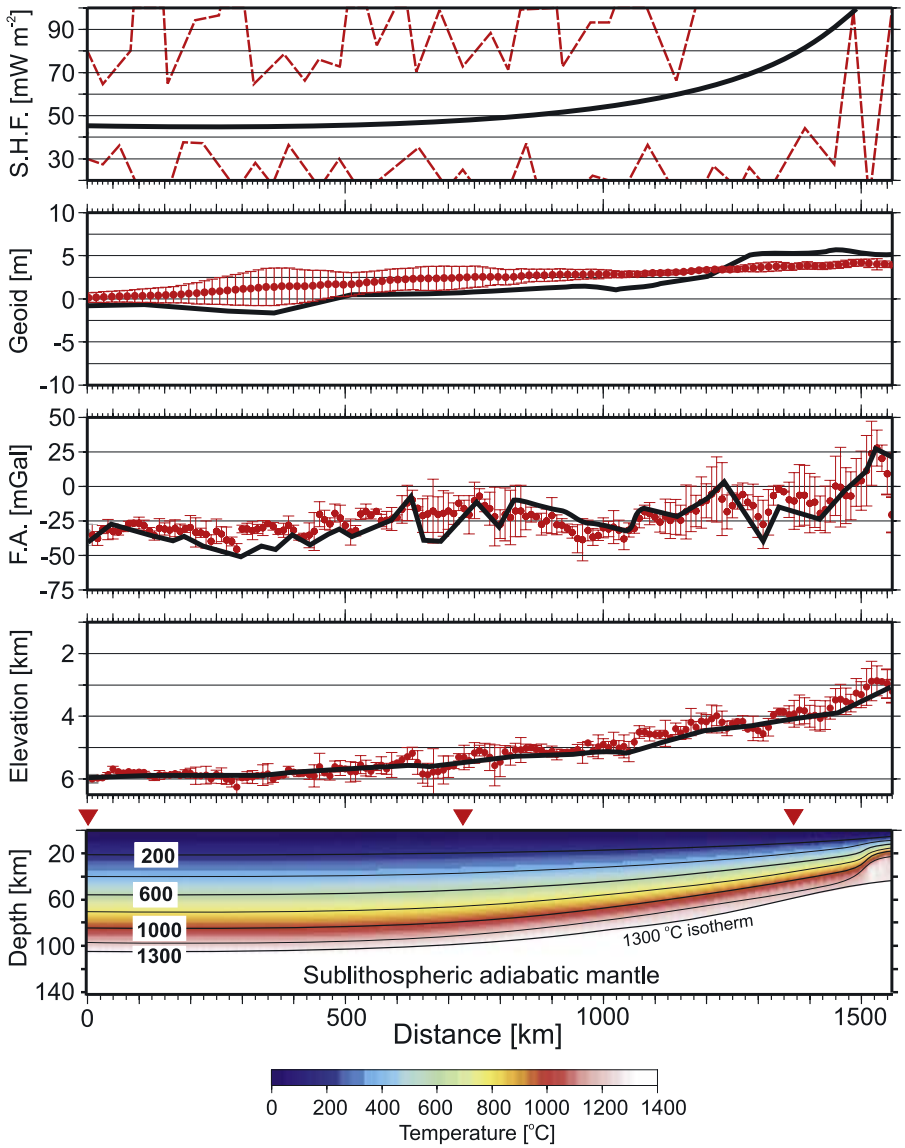

Figure 1. Modelling results of surface heat flow, geoid height, free-air gravity anomalies, and elevation for the transect discussed in the text. The bottom plot shows the thermal structure of the best fitting model. Red triangles mark where the plate is ~90, 40, and 10 Ma old. Red dots and vertical bars denote observed values and associated scatter from global databases along the transect, respectively. Black lines represent outputs from the model. The sharp peaks in the free-air anomaly are a fictitious effect due to the simple one-layer crustal model assumed here. Dashed envelope in the SHF is one standard deviation from the mean value for the global data set of *Stein and Stein* [1992].

depletion between the OL and RM-SI models, which in young plates slightly offsets the negative contribution caused by thermal differences. The effects of the spinel-garnet transition are evident in the two jumps at ~50 and ~76 km depth. The former is the result of the phase transformation taking place within the plate, which is clearly displaced towards deeper levels at younger ages. The latter is a consequence of the downward shifting of the phase transition in the adiabatic RM-SI model. $\Delta\rho$ values >100 kg m^{-3} in the lithospheric mantle are marginally reached in a thin layer below the Moho. Depth-averaged $\overline{\Delta\rho}$ values for the whole plate (i.e., crust included) when depletion is considered in a 90 Ma old plate, is ~35 kg m^{-3}. If the density distribution in a MOR column is used instead as a reference model (i.e., phase changes + partial melting), the above values are increased by only ~5 kg m^{-3}. This is because the density distribution at a MOR exhibits considerable departures from the RM-SI only at depths ≲30 km, where partial melting becomes significant (>5%).

[11] The estimations given above are for a plate generated in a purely passive MOR. Any active component at the time of plate generation would result in a greater average depletion, reducing even more the negative buoyancy of the lithosphere. When this factor is combined with the possible underestimation of the depth of the spinel-garnet transition [*Klemme*, 2004], the $\Delta\rho$ values estimated above are likely to represent upper bounds of attainable $\overline{\Delta\rho}$.

4. Summary and Conclusions

[12] The density structures of unsubducted OL and oceanic sublithospheric mantle have particular relevance

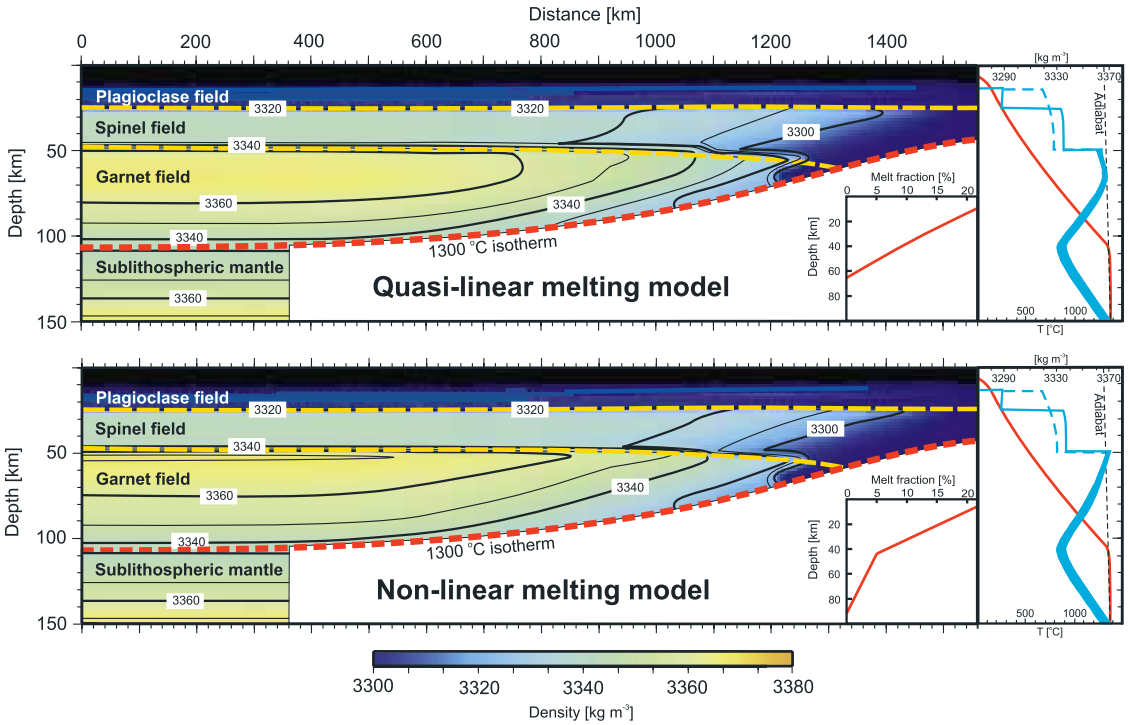

Figure 2. Density structure of the OL assuming both QL and NL depletion models (shown in the insets). The contour lines indicate density values in kg m^{-3}. The dashed yellow lines indicate the approximate locations of the plagioclase-spinel and spinel-garnet phase transitions. The temperature (red) and density (blue) profiles at x = 0 km (~90 Ma) are shown on the right. Areas between solid and dashed lines represent uncertainties due to the plagioclase stability field and thermodynamic parameters; blue bands represent uncertainties due to thermodynamic parameters in the garnet stability field (see supplementary material).

in geodynamic scenarios such as subduction initiation and intraoceanic plate deformation. In this paper we have applied an integrated petrological-geophysical methodology to model the density structure of unsubducted OL and its buoyancy with respect to the underlying mantle. Our results indicate that mature oceanic plates with thermal thicknesses of ~105 ± 5 km do not develop average densities greater than the sublithospheric mantle (i.e., asthenosphere). Also, although the compositional (density) structure of OL makes it statically unstable with respect to the adiabatic mantle after 30 Ma (i.e., positive $\overline{\Delta\rho}$), buoyancy values representative of the whole plate are found to be constrained by $\overline{\Delta\rho} \lesssim 40$ kg m^{-3}, significantly smaller than values used in most models of subduction initiation. The average density and buoyancy of OL is only slightly dependent on the two assumed isentropic melting model at the MOR (QL vs. NL). However, although not explicitly modelled in this paper, different melting models could modify the viscosity structure of OL to a significant extent. Dehydration by melt removal is known to increase the viscosity of olivine by as much as two orders of magnitude [e.g., *Hirth and Kohlstedt*, 1996]. Since fertile mantle with an initial water content of 50–700 ppm becomes virtually dry after only a few percent of melt extraction (5% [e.g., *Asimow et al.*, 2004]), non-linear models with deep tails (i.e., deeper P_o) could generate a thicker high-viscosity layer than typical linear models, making OL more resistant to deformation.

[13] Acknowledging that the generation of new subduction zones is a common feature during the normal evolution of plate tectonics, the results presented in this paper put forward that the intrinsic buoyancy and viscosity structures

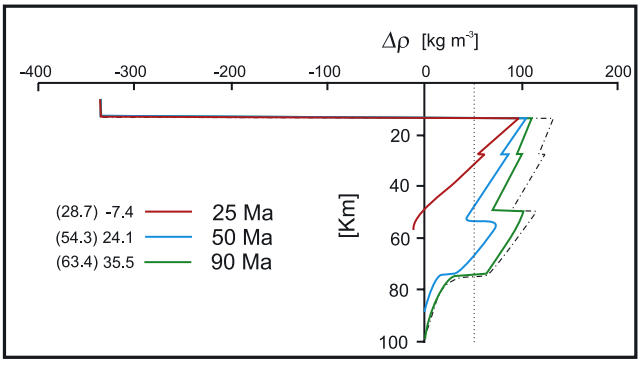

Figure 3. Profiles of density contrast ($\Delta\rho$) with depth between oceanic lithosphere of different ages and adiabatic reference model RM-SI. The vertical thin-dotted line marks the value $\Delta\rho$ = 50 kg m^{-3}. The profile for a 90 Ma old plate with an undepleted composition (i.e., no melt depletion) is also included (thin dashed-dotted line). Values of depth-averaged $\Delta\rho$ in kg m^{-3} are shown for the lithospheric mantle only (numbers within brackets) and for the whole plate.

of OL may not be as critical for initiating subduction as others factors such as localized rheological weakening, external compression, sublithospheric loads, and/or lateral density contrasts [e.g., *Gurnis et al.*, 2004; *Afonso*, 2006]. More generally, the results presented in this paper points to the need of integrating petrological, geochemical, and geophysical modelling to re-examine commonly accepted (and possibly oversimplified) ideas on the evolution of the OL, and to work out the consequences of this re-examination for our understanding of plate tectonic processes.

[14] **Acknowledgments.** We thank W. Griffin and two anonymous reviewers for providing valuable comments on an earlier version of this paper. This work was supported by Carleton U. and OGS scholarships to JCA, a NSERC discovery grant to GR, projects SAGAS-3, WestMed, and ESF-EuroMARGINS to MF.

References

Afonso, J. C. (2006), Thermal, density, seismological, and rheological structure of the lithospheric-sublithospheric mantle from combined petrological-geophysical modelling: Insights on lithospheric stability and the initiation of subduction, Ph.D. thesis, Carleton Univ., Ottawa. (Available at http://wija.ija.csic.es/gt/afonso/homepage.htm.)

Asimow, P. D., M. M. Hirschmann, and L. M. Stolper (2001), Calculation of peridotite partial melting form thermodynamic model of minerals and melts, IV. Adiabatic decompression and the composition and mean properties of mid-ocean basalts, *J. Petrol.*, *42*, 963–998.

Asimow, P. D., J. E. Dixon, and C. H. Langmuir (2004), A hydrous melting and fractionation model for mid-ocean ridge basalts: Application to the Mid-Atlantic Ridge near the Azores, *Geochem. Geophys. Geosyst.*, *5*, Q01E16, doi:10.1029/2003GC000568.

Baker, M. B., and J. R. Beckett (1999), The origin of abyssal peridotites: A reinterpretation of constraints based on primary bulk compositions, *Earth Planet. Sci. Lett.*, *171*, 49–61.

Gurnis, M., C. Hall, and L. Lavier (2004), Evolving force balance during incipient subduction, *Geochem. Geophys. Geosyst.*, *5*, Q07001, doi:10.1029/2003GC000681.

Hacker, B. R., and G. A. Abers (2004), Subduction Factory 3: An Excel worksheet and macro for calculating the densities, seismic wave speeds, and H_2O contents of minerals and rocks at pressure and temperature, *Geochem. Geophys. Geosyst.*, *5*, Q01005, doi:10.1029/2003GC000614.

Hirth, G., and D. L. Kohlstedt (1996), Water in oceanic upper mantle: Implications for rheology, melt extraction and the evolution of the lithosphere, *Earth Planet. Sci. Lett.*, *144*, 93–108.

Hynes, A. (2005), Buoyancy of the oceanic lithosphere and subduction initiation, *Int. Geol. Rev.*, *47*, 938–951.

Klemme, S. (2004), The influence of Cr on the garnet-spinel transition in the Earth's mantle: Experiments in the system MgO-Cr_2O_3-SiO_2 and thermodynamic modelling, *Lithos*, *77*, 639–646.

Klemme, S., and H. S. O'Neill (2000), The near-solidus transition from garnet lherzolite to spinel lherzolite, *Contrib. Mineral. Petrol.*, *138*, 237–248.

Lee, C.-T. A., A. Lenardic, C. M. Cooper, F. Niu, and A. Levander (2005), The role of chemical boundary layers in regulating the thickness of continental and oceanic thermal boundary layers, *Earth Planet. Sci. Lett.*, *230*, 379–395.

McDonough, W. F., and S. Sun (1995), The composition of the Earth, *Chem. Geol.*, *120*, 223–253.

McKenzie, D., J. Jakson, and K. Priestely (2005), Thermal structure of oceanic and continental lithosphere, *Earth Planet. Sci. Lett.*, *233*, 337–349.

Niu, Y. (1997), Mantle melting and melt extraction processes beneath ocean ridges: Evidence from abyssal peridotites, *J. Petrol.*, *38*, 1047–1074.

Niu, Y. (2004), Bulk-rock major and trace element compositions of abyssal peridotites: Implications for mantle melting, melt extraction and post-melting processes beneath mid-ocean ridges, *J. Petrol.*, *45*, 2423–2458.

Schubert, G., D. L. Turcotte, and P. Olson (2001), *Mantle Convection in the Earth and Planets*, Cambridge Univ. Press, Cambridge, U. K.

Schutt, D. L., and C. E. Lesher (2006), Effects of melt depletion on the density and seismic velocity of garnet and spinel lherzolite, *J. Geophys. Res.*, *111*, B05401, doi:10.1029/2003JB002950.

Stein, C. A., and S. Stein (1992), A model for the global variation in oceanic depth and heat flow with lithospheric age, *Nature*, *359*, 123–128.

Turcotte, D. L., and J. Phipps Morgan (1992), The physics of magma migration and mantle flow beneath a mid-ocean ridge, in *Mantle Glow and Melt Generation at Mid-Ocean Ridges*, *Geophys. Monogr. Ser.*, vol. 71, edited by J. Phipps Morgan, D. K. Blackman, and J. M. Sinton, pp. 155–182, AGU, Washington, D. C.

Walter, M. J. (2003), Melt extraction and compositional variability in the mantle lithosphere, in *The Mantle and Core*, *Treatise Geochem.*, vol. 2, edited by R. W. Carlson, pp. 363–394, Elsevier, New York.

J. C. Afonso and M. Fernàndez, Institute of Earth Sciences "J. Almera," CSIC, Luís Solé i Sabarís s/n E-08028, Barcelona, Spain. (jafonso@ija.csic.es; mfernandez@ija.csic.es)

G. Ranalli, Department of Earth Sciences and Ottawa-Carleton Geoscience Centre, Carleton University, 1125 Colonel By Drive, Ottawa, ON, Canada K1S 5B6. (granalli@earthsci.carleton.ca)